Available online at www.sciencedirect.com
SCIENCE DIRECT®
Nuclear Engineering and Design 224 (2003) 105–117
Nuclear Engineering and Design
www.elsevier.com/locate/nucengdes

Advanced flaw production method for in-service inspection qualification mock-ups

Mika Kemppainen [a,*], Iikka Virkkunen [a], Jorma Pitkänen [b], Raimo Paussu [c], Hannu Hänninen [d]

[a] *Trueflaw Ltd., P.O. Box 540, FIN 02151 Espoo, Finland*
[b] *VTT Industrial Systems, Espoo, Finland*
[c] *Fortum Nuclear Services Ltd., Espoo, Finland*
[d] *Helsinki University of Technology, Espoo, Finland*

Received 21 October 2002; received in revised form 27 February 2003; accepted 8 March 2003

Abstract

One of the key issues in in-service inspection qualification is the representativeness of the defects used in qualification specimens. The best representativeness is achieved with realistic defects. However, present specimen production techniques have some significant weaknesses, such as unrealistic defects or additional alterations induced in the surrounding material. Specimens manufactured, for example, by weld implantation or with weld solidification defects always result in one or more extra weld interfaces. These interfaces can be detected by NDT. To overcome problems with the current specimens, a new defect manufacturing technique was developed. The new technique produces natural, representative defects without introducing additional weld metal or other unwanted alterations to the specimen.

The new method enables artificial production of single, separate fatigue cracks by thermal loading. The method is based on a natural thermal fatigue damage mechanism and enables production of real cracks directly into the samples. Cracks are produced without welding or machining and without any preliminary surface treatment or artificial initiator such as a notch or a precrack. Single crack or a network of cracks can be induced into the base material, welded areas, HAZ, weld claddings, threaded areas, T-joints, etc. The location, orientation and size of produced cracks can be accurately controlled. Produced cracks can be used to simulate different types of service-induced cracks such as thermal fatigue, mechanical fatigue and stress corrosion cracks. It is shown that artificially produced thermal fatigue cracks correspond well with the real, service-induced cracks and overcome the problems of traditional qualification specimen manufacturing techniques.

1. Introduction

Thermal fatigue, that is, material degradation due to successive temperature changes, is one of the life-limiting mechanisms in nuclear power plant conditions. During the operation of a power plant thermal fatigue cracks can initiate and grow in various components. Causes for this are mixing, striping or stratification of hot and cold water (Hytönen, 1998).

* Corresponding author. Tel.: +358-45-6354414; fax: +358-9-455-3117.
E-mail addresses: mika.kemppainen@trueflaw.com (M. Kemppainen), iikka.virkkunen@trueflaw.com (I. Virkkunen), jorma.pitkanen@vtt.fi (J. Pitkänen), raimo.paussu@fortum.com (R. Paussu), hannu.hanninen@hut.fi (H. Hänninen).

0029-5493/$ – see front matter © 2003 Elsevier Science B.V. All rights reserved.
doi:10.1016/S0029-5493(03)00078-5

A typical component, where thermal fatigue cracking occurs, is a T-joint where hot and cold fluids meet and mix. The turbulent mixing of fluids with different temperatures induces rapid temperature changes to the pipe wall. The resulting uneven temperature distribution prevents thermal expansion and gives rise to thermal stresses. The successive thermal transients cause varying, cyclic thermal stresses. These cyclic thermal stresses cause fatigue crack initiation and growth similar to cyclic mechanical stresses. (Virkkunen, 2001).

Cracks occur in nuclear power plant components in different locations such as in straight pipe sections, valve bodies, pipe elbows, collector head screw holes, etc., as well as in base material and in weld joints (ASME, 1990). Crack growth direction depends on the component and the location, based on the local shape effect and the loading conditions. Pipe cracks can grow both axially and circumferentially, in weld joints both parallel to the weld in the heat-affected zone (HAZ) and transverse to the weld, in threads both vertically and horizontally.

Thermal stresses are typically equi-biaxial and they are highest at the loaded surface. The loading is strain controlled and very high local stresses can arise. If the stresses locally exceed the yield strength of the material, thermally induced residual stresses arise (Virkkunen et al., 2000). Due to the high surface stresses, the thermal fatigue cracks often form a mosaic-like crack pattern of shallow cracks. There have been several incidents showing that some of the shallow cracks extend deeper into the material and can grow through the wall thickness (ASME, 1990; Hänninen and Hakala, 1981).

During the in-service inspections thermal fatigue cracks create a challenge for ultrasonic inspection, both for detection and sizing. The difficulty of the inspection is caused by the characteristics of the cracks, which cause the ultrasonic energy to diffuse, attenuate, scatter, diffract, etc. (Becker et al., 1981). Typical characteristics affecting the ultrasonic inspection are crack opening (Yoneyama et al., 2000), fracture surface roughness (Ogilvy, 1989), branching (Wirdelius and Österberg, 2000), residual stress (Iida et al., 1988), plastic zone (Saka and Fukuda, 1991), etc. Each of these factors affects the performance of ultrasonic testing. Therefore, it is crucial to identify the key characteristics of service-induced and artificially induced flaws and to understand how they affect the ultrasonic response obtained during inspection.

The most effective in-service inspection qualification is achieved with qualification specimens, which are as representative as possible of all service conditions. In order to have similar physical reflector to that of service-induced crack, it is commonly understood that real or realistic cracks must be used in the in-service inspection qualification mock-ups. Problems with the artificial defect incorporation methods have, so far, restricted the use of realistic cracks in qualification mock-ups. The developed method that is described in this paper allows controlled production of realistic cracks that have NDE responses similar to service-induced cracks.

In this paper, the performance of the new method for producing artificial flaws with thermal fatigue is demonstrated and validated using the results of destructive and non-destructive tests. Destructive tests reveal typical metallographic characteristics of produced cracks. Metallographic results are compared to corresponding service-induced cracks documented in the open literature. Non-destructive results are compared to corresponding results from EDM-notches and real, service-induced cracks. The feasibility of the method is demonstrated by three different cases where artificial defects have been produced in real components.

2. Experimental

Different test samples were produced in order to verify the new crack production method. Samples were studied both non-destructively and destructively. Thermal fatigue loading was applied with high frequency induction heating and water or air cooling in order to achieve high heating and cooling rates. Controlled initiation and growth of cracks were followed by replica assisted light optical microscopy. Ultrasonic examinations were performed to determine the non-destructive response of the cracks produced. Destructive testing and scanning electron microscopy were carried out to study the microstructural propagation and fracture surface morphology. Ultrasonic response as well as metallographic properties of artificial cracks were compared to properties of real, service-induced cracks.

The manufacturing process employed does not require any crack starter or artificial initiator and it is

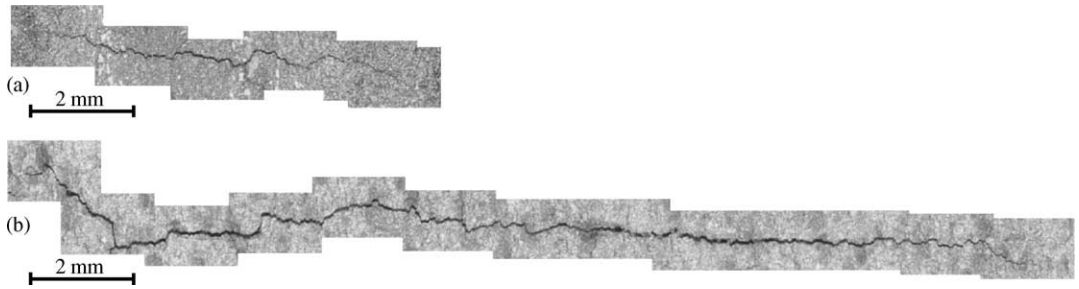

Fig. 1. Two surface breaking thermal fatigue cracks: (a) surface length approximately 8 mm (30,021 thermal fatigue cycles) and (b) surface length approximately 20 mm (166,971 thermal fatigue cycles) in AISI 304 type austenitic stainless steel plate.

applied to the actual surface of a component. Consequently, the process does not leave any unwanted alterations to the material, which may be detected in ultrasonic or eddy current examination.

Crack properties affecting the non-destructive examination include among others: location and orientation, microstructural propagation, branching, crack opening/closure and surface roughness (R_z) of the crack and the shape of the crack tip. These parameters affect both detection and sizing of service-induced cracks. After characterising the properties of artificially produced thermal fatigue cracks they were compared to corresponding properties of real, service-induced thermal fatigue cracks.

The new defect production method utilises the same, natural thermal fatigue damage mechanism, which is also present in real components. The method enables controlled defect production in similar locations and directions as those where real cracks occur. For the artificial crack production, there are no limitations for component shape or size, or for crack orientation or location.

2.1. Microscopy

In austenitic stainless steels thermal fatigue cracks initiate from slip bands. From the multitude of initial microcracks one single crack can be grown by controlled thermal loading. In Fig. 1 there are two examples of artificially produced surface breaking cracks. Cracks follow the crystallographic path through the microstructure. The crack path is tortuous, but the macroscopic surface crack growth follows the predetermined direction. In Fig. 2, cross-sections of two different cracks are shown, where tortuous and transgranular crack propagation can be seen. The propagation is different for each crack because these cracks were produced with different thermal fatigue parameters. The cracks show minor branching, they are narrow and the crack tip radii are small.

The crack depth is controlled cycle-by-cycle as the produced crack depth depends on the magnitude of the applied thermal cycle and the total number of cycles. Artificially produced cracks have rough fracture surfaces where the per-cycle crack extension

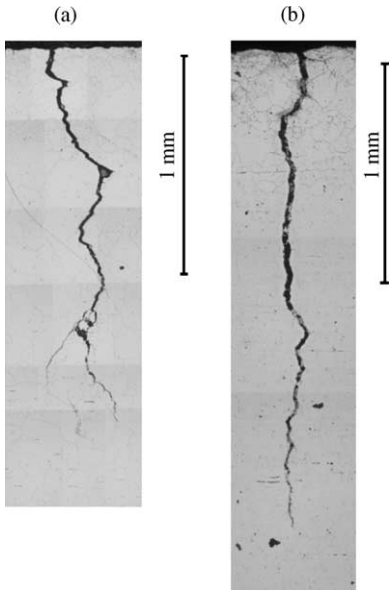

Fig. 2. Cross-sections of two artificially produced thermal fatigue cracks in AISI 304 type austenitic stainless steel with different fracture surface roughness resulting from different production parameters. Cracks after (a) 30,000 thermal fatigue cycles and (b) 2770 thermal fatigue cycles.

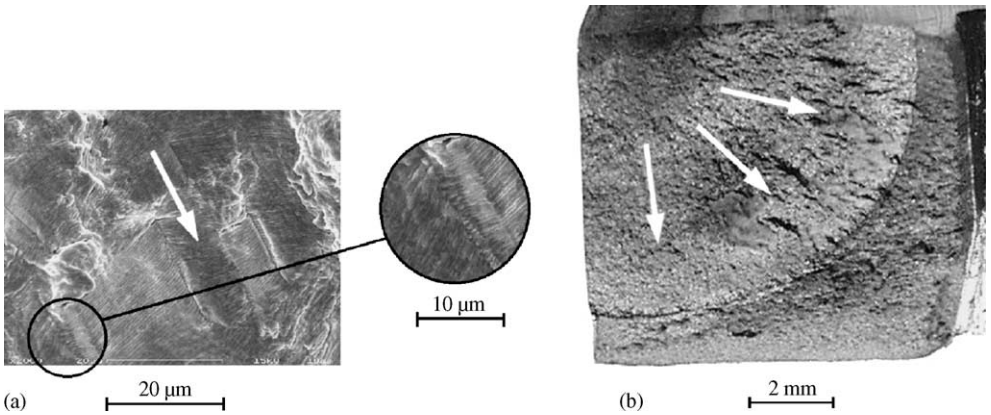

Fig. 3. Artificially produced thermal fatigue crack (a) has fatigue striations on the fracture surface and (b) follows elliptical shape in its growth (82% of the wall thickness penetrating crack). White arrows show crack growth directions. Material is AISI 304 type austenitic stainless steel.

can be followed from the fatigue striations. Each striation represents an incremental advance of the crack front during one load cycle. The magnitude of the increment, that is, striation spacing, depends on the stress/strain range. Typically the striation spacing varies in different areas of the crack. In a small crack the spacing is small, but it increases as the crack gets bigger. The crack growth follows an elliptical shape, which in the limit approaches a circular configuration. Typical fracture surface and shape of a big crack are shown in Fig. 3. The white arrows in the picture show the crack growth direction. In Fig. 3b half of the fracture surface of an 82% through wall thickness (7 mm deep) crack is shown. The initiation surface, that is, pipe inner surface, is in the upper part of the figure and the outer surface of the sample pipe is shown in the lower part of the figure.

2.2. Metallographic comparison of artificially produced and service-induced thermal fatigue cracks

The non-destructive response reveals the microstructural characteristics of the service-induced crack. In order to have similar non-destructive response, artificially produced cracks should simulate the microstructural properties of service-induced cracks. In Fig. 4, a service-induced and an artificially produced thermal fatigue crack are presented side by side.

The macroscopic propagation of real and artificially produced thermal fatigue cracks is similarly tortuous. As shown in Fig. 4, both cracks are narrow, propagate transgranularly in the microstructure and show minor branching. The real, service-induced crack has the larger opening or width near the surface and it is tight in the vicinity of the crack tip. The typical crack surface width of a service-induced thermal fatigue crack in austenitic stainless steels varies between 5

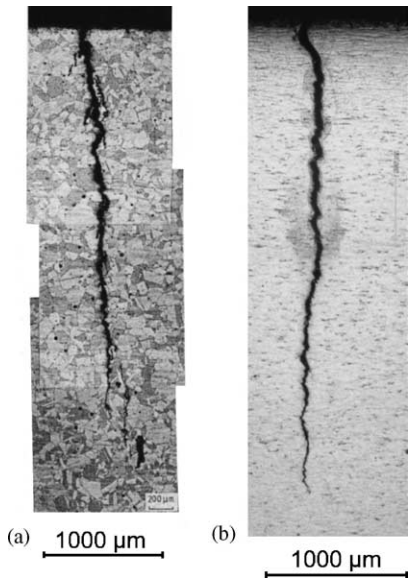

Fig. 4. Comparison of cross-sections of (a) a service-induced (Hänninen and Hakala, 1981) and (b) an artificially produced thermal fatigue crack (6500 thermal fatigue cycles).

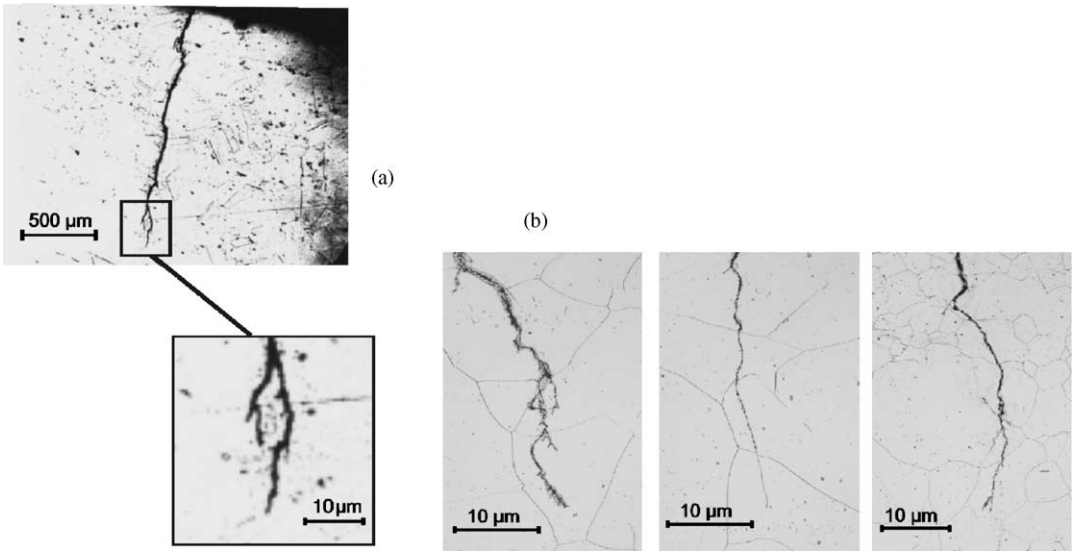

Fig. 5. Comparison of crack tips of (a) a service-induced (Wåle and Ekström, 1995) and (b) three artificially produced thermal fatigue cracks (after 30,000 thermal fatigue cycles).

and 380 μm, at one half the through wall depth of the crack between 2 and 190 μm and at the crack tip between 1 and 18 μm (Wåle and Ekström, 1995). The opening of a crack is affected by many factors including the condition of the residual stress along the fracture surface. Fracture surface of a service-induced thermal fatigue crack is rough. Typical surface roughness (R_z) values in austenitic stainless steels

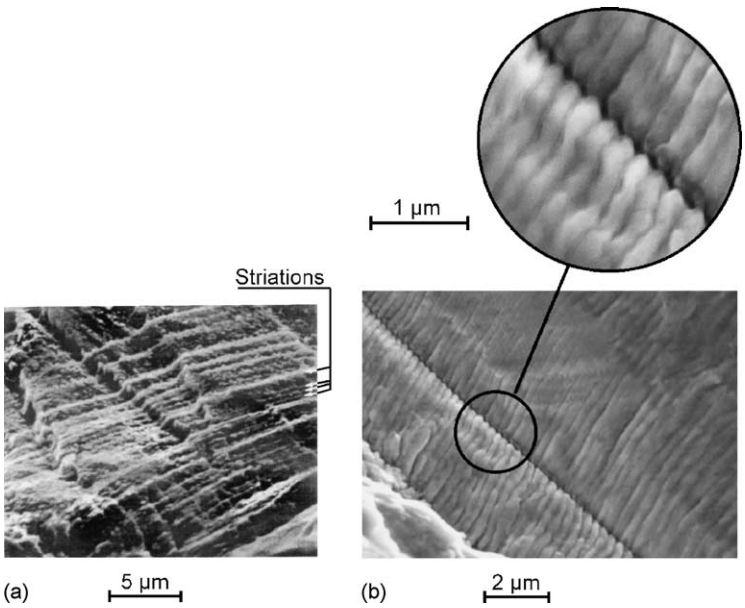

Fig. 6. Comparison of fracture surfaces of (a) a service-induced (Pirson and Roussel, 1998) and (b) an artificially produced thermal fatigue crack.

vary between 6 and 140 μm (Wåle and Ekström, 1995).

In Fig. 4 the artificially produced thermal fatigue crack has a similar opening behaviour to that of the service-induced crack. The approximate width of the artificially produced thermal fatigue crack is 70 μm at surface, in the middle-section 40 μm and at the crack tip 2 μm. Typical values of surface roughness (R_z) for artificially produced thermal fatigue crack varies between 35 and 125 μm. Surface roughness was calculated digitally from cross-sectional images. The difference of height between ten highest peaks and ten lowest valleys on the fracture surface were measured for each image and the average of measurement results was reported as R_z.

The tortuous crack path has formed when the crack propagation direction changes crystallographically at grain boundaries in the microstructure. Fig. 5 shows a comparison of crack tips of service-induced and artificially produced thermal fatigue cracks.

The crack tip of a service-induced thermal fatigue crack has typically a very small radius and crack surfaces near the tip are close to each other, which is shown in Fig. 5. The tip of artificially produced thermal fatigue cracks is similarly tight and has a very small radius. Fatigue crack growth can be followed from the fracture surface from fatigue striations. In Fig. 6, a comparison of striations on fracture surfaces of a service-induced and an artificially produced thermal fatigue crack is shown.

Striations on the fracture surfaces of service-induced and artificially produced thermal fatigue cracks are similarly visible, as shown in Fig. 6. The cycle-dependent incremental crack growth makes it possible to control the artificial crack production accurately.

2.3. Non-destructive testing

Artificially produced thermal fatigue cracks in austenitic stainless steel pipe base material and austenitic stainless steel strip welded cladding were characterised by ultrasonic and eddy current methods. The objective of ultrasonic measurements was to study the detectability of artificially produced thermal fatigue cracks and to characterise the cracks from the ultrasonic signal point of view. Characterisation included studying the ultrasonic signal obtained from crack corner reflection effect, fracture surface and crack tip. Additionally, the variation of ultrasonic signal from different areas of the crack was studied. The objective of using the eddy current method was to study the detectability and sizing capability in austenitic stainless steel cladding.

2.3.1. Base material

Two cracks were produced (one in axial and the other in circumferential directions) in austenitic stainless steel pipe base material (Fig. 17). The diameter of the pipe was about 360 mm and wall thickness 28 mm. Both cracks were placed in the inner surface of the pipe. The surface length of the circumferential crack was 20 mm and depth approximately 6 mm. The length of the axial crack was 20.5 mm and depth approximately 3 mm.

Cracks in the base material were characterised ultrasonically with longitudinal, transverse and secondary creeping waves. Two techniques with longitudinal waves, 0°L (longitudinal) 5 MHz single element probe and ADEPT60°L 3 MHz dual element special probe, were used. With transverse waves two different 2 MHz composite probes (MWK 45-2 and MWK

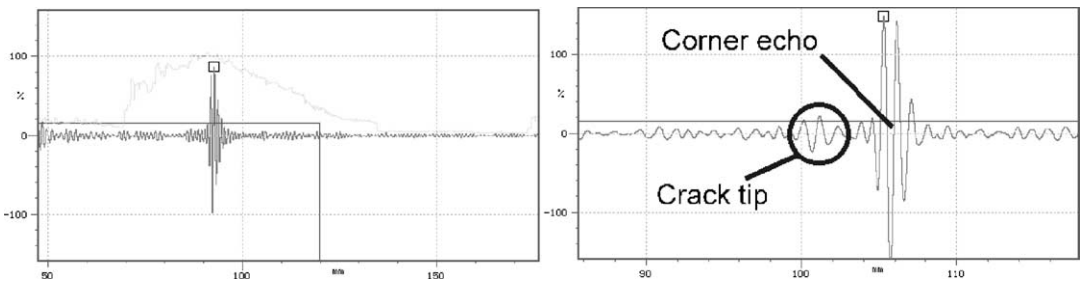

Fig. 7. Ultrasonic A-scans (time–amplitude) from an artificially produced circumferential thermal fatigue crack obtained with 70°T probe (MWK 70-2E).

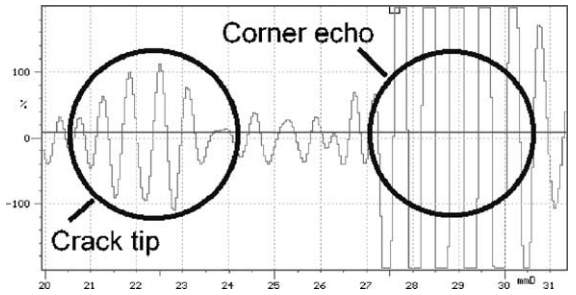

Fig. 8. Ultrasonic A-scan from an artificially produced circumferential thermal fatigue crack obtained with 45°T probe (MWK 45-2).

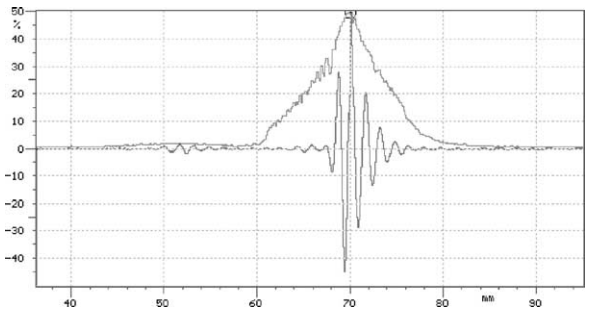

Fig. 9. Ultrasonic corner echo dynamics from an artificially produced circumferential thermal fatigue crack obtained with secondary creeping wave probe (WSY 70-2).

70–2E) and 2 MHz mode conversion probes (WSY 70-2) were used. The inspection results obtained using these different probes from artificially produced circumferential crack are shown in Figs. 7–10.

In the austenitic stainless steel base material the tip of circumferential crack was detected with both types of ultrasonic longitudinal wave probes as shown in

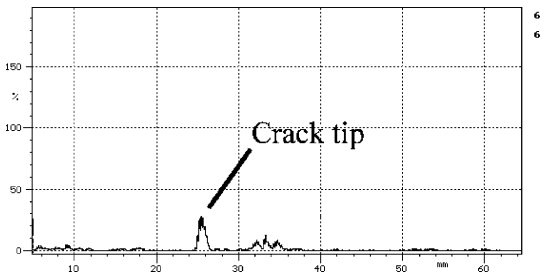

Fig. 10. Ultrasonic A-scan from an artificially produced circumferential thermal fatigue crack obtained with mode conversion probe (ADEPT60°L).

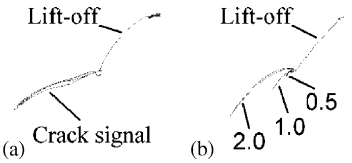

Fig. 11. Eddy current signal from (a) an artificially produced thermal fatigue crack in austenitic stainless steel strip welded cladding and (b) three EDM-notches (depths 2.0, 1.0 and 0.5 mm) in austenitic stainless steel base material.

Fig. 15 (0°L) and Fig. 10 (ADEPT60°L). However, with 0°L no proper echo from the crack face was detected. With transverse waves, echoes from crack tips were detected both with 70°T (S/N approximately 10 dB) and 45°T (S/N approximately 15 dB) 2 MHz probes (Figs. 7 and 8, respectively). The obtained signal-to-noise ratio results show that with transverse waves the crack tip was more clearly seen with the 45° probe than with 70° probe.

During ultrasonic testing with the mode conversion probe (Fig. 9) the received secondary creeping wave echo from the transverse crack disappeared locally. This is caused most likely by a discontinuous crack extension or local compressive residual stress, which presses the crack surfaces closely together, thus enabling ultrasonic waves to penetrate through the crack.

2.3.2. Cladding

One crack was produced in a strip welded AISI 316 type austenitic stainless steel cladding of a ferritic steel test block (465 mm × 150 mm × 100 mm, length × width × height). The cladding was 10 mm thick and the produced crack was about 10 mm long and 3 mm deep. Three different size (depths 0.5, 1.0 and 2.0 mm) of rectangular (70 mm long and 0.3 mm wide) EDM-grooves used for eddy current calibration were produced in a separate austenitic stainless steel plate.

The eddy current inspection was performed with a 100 kHz probe (Zetec 195-801P02 Fe). The crack was detected in the cladding, although the impedance level varied depending on the δ-ferrite content and the probe location on the strip welded cladding (middle of strip, HAZ, fusion line). The crack was estimated to be about 3 mm deep. Fig. 11 shows eddy current signals from the artificially produced crack and from three different EDM-grooves used for calibration. Also the

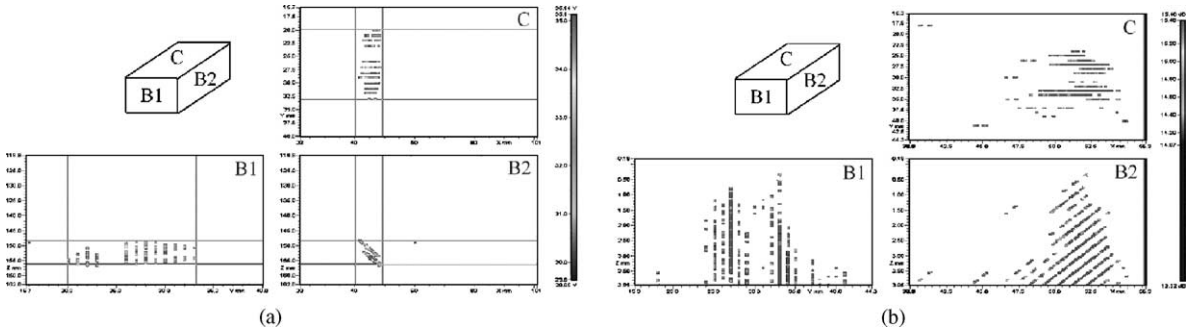

Fig. 12. Ultrasonic testing results of an artificially produced thermal fatigue crack in austenitic stainless steel cladding: (a) from outside surface with long sound path with 41°T (1 MHz) wave probe and (b) from crack opening surface with 70 TRL (2 MHz) wave probe.

sizing results of eddy current testing may be affected by the possible compressive residual stress affecting the crack tip.

Ultrasonic inspection of the cladding sample was performed from the crack opening surface (with 70°TRL, 2 MHz probe) and with a long sound path (about 200 mm) from the outside surface of the test block (with 41°T, 1 MHz probe). The results in Fig. 12 show two ultrasonic B-scans in the bottom line and one C-scan above them. The orientations of scan directions are visualised in the figure. The crack was detected from both sides of the test block, but no crack tip echo was detected in either case. This is explained by the limited resolution of the probing frequencies used and a possible compressive residual stress closing the crack tip.

2.4. Non-destructive comparison of artificially produced and service-induced thermal fatigue cracks

The non-destructive testing results obtained from artificially produced thermal fatigue cracks were compared to the results obtained with an EDM-notch and a real service-induced thermal fatigue crack. The service-induced thermal fatigue crack was caused by mixing of fluids at different temperatures in a T-joint process pipe. The cracked area was found based on pipe leakage. By closer inspection, numerous transversal cracks were found, one of them penetrating through the wall of the pipe. A 13 mm deep crack was selected to be used in this study.

The objective of the comparison of different reflectors was to show the difference between ultrasonic responses obtained. The inspection of all three different types of reflectors was performed during the same session with the same equipment and personnel. The artificial thermal fatigue crack was produced in the same pipe containing the service-induced crack. The pipe material was AISI 321 type austenitic stainless steel (Ti-stabilised). The third reflector, a semi-elliptical EDM-notch, was in a separate plate (thickness 30 mm) of AISI 316 type austenitic stainless steel.

Crack tip echoes obtained with 0°L 5 MHz single probe from the EDM-notch, the service-induced thermal fatigue crack and the artificially produced thermal fatigue crack are presented in Figs. 13–15, respectively. The crack tip echo is clearly seen from EDM-notch but from the real and artificially produced thermal fatigue cracks the S/N ratio is low, being about 6–10 dB. However, the S/N ratios of crack tip signals were about the detection limit value (6 dB). With artificially produced thermal fatigue crack the crack tip signal was not equally clear over the whole length of the crack. The signal shown in Fig. 15 is from an area where the crack tip signal was optimal.

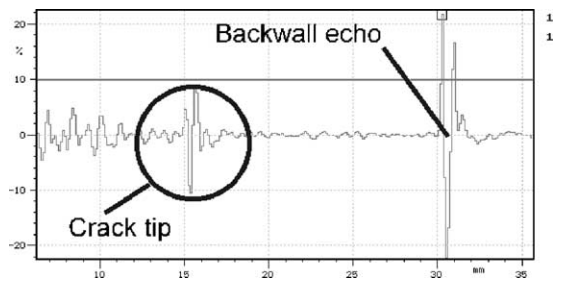

Fig. 13. Ultrasonic A-scan of a 15 mm deep semi-elliptical EDM-notch in AISI 316 type austenitic stainless steel (V110-0°L).

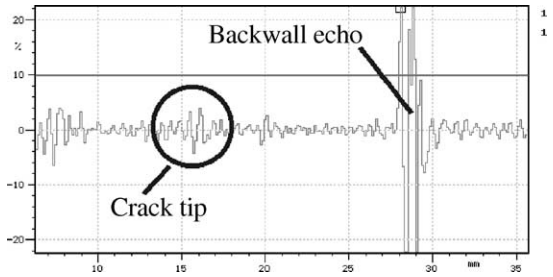

Fig. 14. Ultrasonic A-scan of a 13 mm deep real, service-induced thermal fatigue crack in AISI 321 type austenitic stainless steel (V110-0°L).

2.5. Residual stress

Residual stress state affects the opening of the produced crack, which in turn affects the reflection and transmission behaviour of the ultrasonic energy. Residual stress can be measured on the surface of the sample with relative ease, while measurement through the thickness of the sample near a crack is difficult. Fig. 16 shows an example of cumulative change of surface residual stress caused by continued thermal fatigue cycling. Residual stresses were measured in two directions during test interruptions when the sample had cooled down to room temperature. During the test, an individual, 8 mm long crack was produced with a total of 35,000 cycles. Residual stress measurements were performed in the mid-section of the crack in the solid material, 1 mm away from the crack opening. Measurements were done with X-ray diffraction, which reveals stresses from a thin surface layer (thickness 15–30 μm). Measurements were performed with Cr radiation, 3 mm (diameter) collimator and 60 s exposure time. Residual stress measurements through the thickness of the sample were not performed in this study.

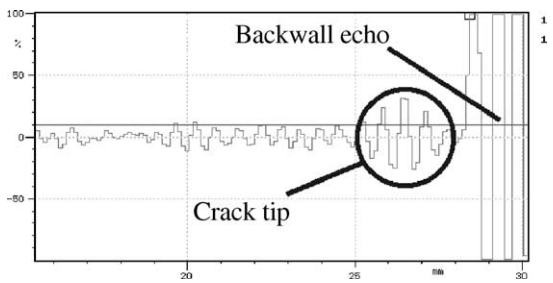

Fig. 15. Ultrasonic A-scan of an artificially produced circumferential 20 mm long and approximately 6 mm deep thermal fatigue crack in AISI 321 type austenitic stainless steel (V110-0°L).

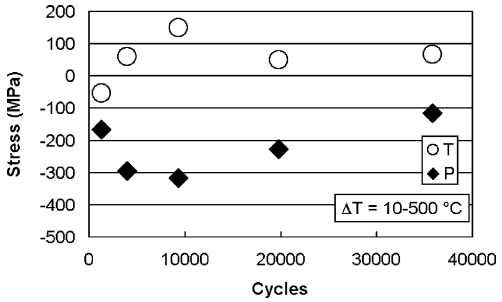

Fig. 16. Change of surface residual stresses as a function of continued thermal fatigue cycling in the vicinity of crack produced in AISI 304 type austenitic stainless steel plate (T: stresses transverse to the crack, P: stresses parallel to the crack).

The change of surface residual stresses in Fig. 16 demonstrates that the applied thermal fatigue cycle has a strong effect on the final residual stress distribution. Residual stress transverse (marked as "T") and parallel (marked as "P") to the crack show opposite behaviour as transverse stress moves very quickly in tension and parallel stress in compression. In this example thermal cycling was controlled so that the crack opening is pronounced, that is, transverse stress was set in tension. Thus, by controlling the thermal cycling also the residual stresses can be controlled.

2.6. Real components

The developed defect production method works well both from the metallographical and non-destructive response point of view. A further interest was to verify the applicability of the method to real components. Verification has been done with different types of components: pipe section, butt-welded pipe, T-joint of two pipes and a collector head threaded screw hole. Materials have been different types of austenitic stainless steels. Results of these tests are presented in the following.

2.6.1. Pipes

Three different sizes of pipes were examined during the experiments. Cracks were produced on the inner surface of the pipes. In Fig. 17 is an example of a pipe (diameter approximately 360 mm, wall thickness

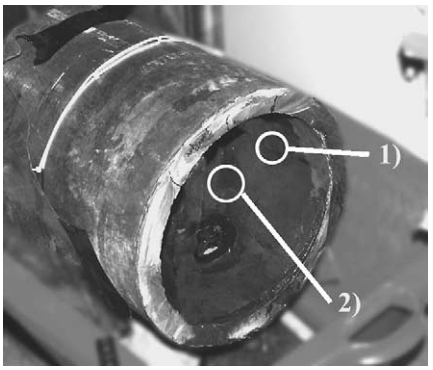

Fig. 17. Austenitic stainless steel pipe: (1) circumferential 20 mm long and (2) axial 20.5 mm long artificially produced thermal fatigue crack (89,200 and 112,820 thermal fatigue cycles, respectively) (pipe diameter 360 mm, wall thickness 28 mm).

28 mm) on the inner surface of which one circumferential and one axial thermal fatigue crack were produced. The cracks were produced in the base material with lengths of about 20 mm. In another case, a crack was produced in the inner surface of a 159 mm × 8.5 mm (diameter × wall thickness) pipe. The crack was 82% of the wall thickness being about 7 mm deep (Fig. 3). Additionally, cracks have been produced in the heat affected zones of butt-welded pipes.

2.6.2. T-joint of pipes

Artificially produced thermal fatigue cracks were produced in the corner of a T-joint of pipes of different sizes (110 mm × 20 mm and 570 mm × 35 mm). Neither surface nor any other pre treatment was performed on this area. Two individual cracks were produced in the desired locations with location accuracy of

Fig. 18. Production of artificial thermal fatigue cracks inside of austenitic stainless steel collector head threaded screw hole.

±1° and length sizing accuracy of ±0.3 mm (surface length).

2.6.3. Collector head

The method was applied to a piece of a VVER steam generator collector head that had previously been in use in a nuclear power plant. The piece included three threaded holes (diameter 48 mm) with a bottom cup in the end of the holes. Artificial cracks were produced in the threaded area and the bottom cup area. Cracks produced in the threaded area were used as initiating flaws for subsequently growing transgranular stress corrosion cracks. A general picture of the collector head mock-up is shown in Fig. 18. The arm of the induction heater is shown in the left side hole of the figure. An example of a horizontal crack produced at the bottom of a thread is shown in Fig. 19. The crack has first initiated by thermal fatigue mechanism and then grown further by stress corrosion. During the production of the horizontal crack shown, a vertical crack developed.

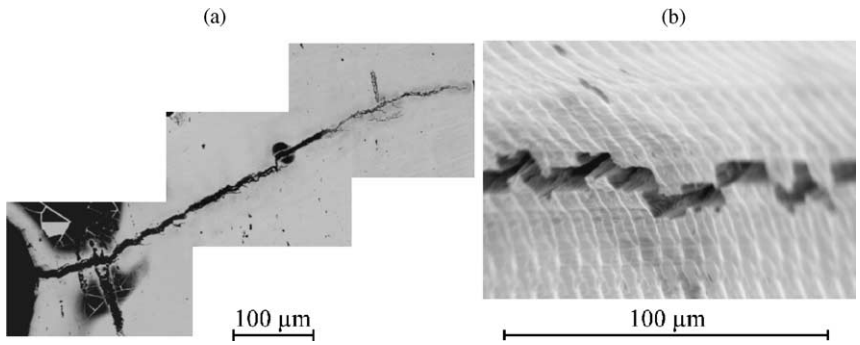

Fig. 19. Artificial thermal fatigue crack at the bottom of a thread: (a) cross-section and (b) crack opening on the surface of the thread bottom.

3. Discussion

Production of realistic thermal fatigue cracks is based on controlled, cyclic thermal loading. During the manufacturing process, varying heating and cooling periods are applied in order to control the thermal stresses induced. Single thermal fatigue cracks first initiate and then grow. There are a wide variety of thermal fatigue cracks, which can be produced by this method. These are single cracks with, for example, different fracture surface roughness, different tortuous crack paths, many or few branches, different growth directions (e.g. when compared to rolling direction of a plate), different aspect ratios (depth to length ratios), different states of residual stresses, etc. Furthermore, it is possible to grow combinations of single cracks, as parallel cracks, intersecting cracks or several cracks forming a network.

The crack path of the artificially produced thermal fatigue crack is tortuous. Tortuous path is a result of the natural crack growth mechanism. The produced thermal fatigue crack has rough fracture surfaces exhibiting clear fatigue striation formation and typically crack has a semielliptical shape.

Thermal loading exceeding the yield strength of the material causes residual stresses. The applied cyclic thermal loading and the number of cycles determine the magnitude of the residual stress. Thus, the residual stress near the crack, along the crack length and path, can be controlled by controlling the applied thermal loading. It is commonly known, that the ultrasonic signal obtained from a crack is affected by the stresses present in the vicinity of the produced crack (Iida et al., 1988; Yoneyama et al., 2000). According to Wirdelius and Österberg (2000), for example, 200 MPa increase in the closing pressure of a flaw causes 10 dB drop in ultrasonic signal amplitude. Changes in the residual stresses along the crack path (at the crack tip, in the middle of the crack and near the crack mouth) affect the ultrasonic energy penetration in different locations. These changes increase the uncertainty of the signal analysis and affect flaw detection and the difficulty of sizing flaws accurately.

The artificially produced cracks realistically simulate the real, service-induced cracks from the metallurgical and ultrasonic point of view. Metallurgically the produced cracks are narrow, have a rough fracture surface, show minor branching, propagate transgranularly and have a tight crack tip with a small radius. Artificially produced thermal fatigue cracks do not have an oxide layer on their fracture surface, as is the case with the service-induced cracks. However, an oxide layer can be grown by a subsequent heat treatment.

Artificially produced thermal fatigue cracks gave similar ultrasonic responses compared to real service-induced cracks (corner echo, crack tip, fracture surface). Studied cracks in austenitic stainless steel base material pipe were reliably detected and sized. No additional cracks were detected near the produced cracks. Crack in the austenitic stainless steel cladding was detected easily, but no crack tip echo was detected which makes the sizing of the crack difficult. This may be caused by compressive stresses affecting the crack tip. The possible compressive stress at the crack tip may also affect the use of eddy current-based crack sizing. Further, the inhomogeneous welded cladding caused some uncertainties in eddy current inspection.

The ultrasonic signal amplitudes from a service-induced and artificially produced thermal fatigue cracks are not as high as those obtained from an EDM-notch. A reason is that the ultrasonic reflectivity is affected by the rougher reflection surface and the narrow opening (width) of the cracks, while the EDM-notch has a smoother reflection surface and is relatively wide. The tip of the EDM-notch gave a clear and sharp signal, while the signals from crack tips were formed by multiple signals produced by the irregularities of the crack tips. Furthermore, the possible stresses present at the crack tips may affect

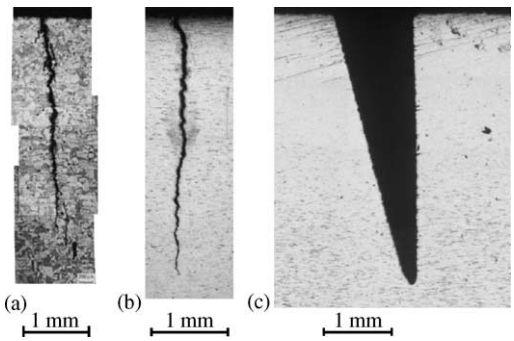

Fig. 20. Comparison of (a) a service-induced thermal fatigue crack (Hänninen and Hakala, 1981), (b) an artificially produced thermal fatigue crack and (c) an EDM-notch (modified PISC type A).

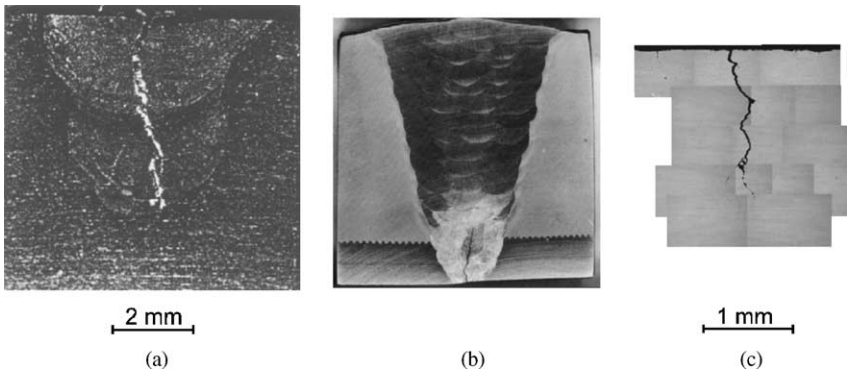

Fig. 21. Comparison of defects produced with different techniques: (a) a weld solidification crack (Watson and Edwards, 1996), (b) a surface breaking crack in a weld (Uddcomb, 1999) and (c) an artificially produced surface breaking thermal fatigue crack.

the ultrasonic signals, while the tip of an EDM-notch is stress free. In this study, the crack tip of an artificially produced thermal fatigue crack in austenitic stainless steel base material was detected by several probes and the crack tip echo had similar S/N ratio as obtained from real service-induced thermal fatigue cracks. Fig. 20 illustrates the difference between the service-induced crack, artificially produced crack and modified PISC type A EDM-notch.

Controlled thermal fatigue cracks are produced without causing any additional alterations in the surrounding material. As an example Fig. 21 compares defects produced by two other qualification defect production techniques and the new artificial thermal fatigue crack production method.

Fig. 21 shows that the other techniques introduce additional weld metal volume, while controlled production of thermal fatigue cracks results precisely in the desired crack without any alterations in the surroundings. During the production of artificial thermal fatigue cracks only a small area of interest is loaded. Consequently the size of the specimen is irrelevant to the production method and cracks can be produced in very large components.

The artificial crack production method has been applied to different nuclear power plant components: pipes, T-joints of pipes and collector head samples. Materials have been austenitic stainless steels commonly used in the nuclear power plants. So far, practically no limitations have been met for the applicability of the method. The only requirement for the applicability is that the location where the crack is to be produced must be accessible for the induction heating coil.

4. Conclusions

A new artificial flaw production method for NDT-qualification defect production purposes has been developed. The method is based on controlled thermal fatigue loading. The flaw production can be controlled so that the location, orientation and size of the cracks are accurately adjusted. Single cracks are grown without any additional alterations caused in the material. Cracks can be produced in base material or welded areas, in simple plate samples or full scale mock-ups. It is shown that artificially produced cracks correspond well with the service-induced cracks both non-destructively and destructively.

Artificial, representative cracks can be produced in samples and mock-ups of different sizes and shapes. The experiments performed proved that artificial surface breaking thermal fatigue cracks can be induced in any component with practically no limitations in location, orientation or size. With this method realistic, controlled cracks can be produced in new mock-ups, in existing mock-ups containing other defects or the method can be used to grow further existing defects of different types. The method is also applicable to change the opening and the residual stress state of an already existing real crack.

Acknowledgements

The main part of the work was carried out at Helsinki University of Technology as a post-graduate study financed by Foundation of Walter Ahlström, Foundation of Runar Bäckström and Technology Development Foundation (TES). The rest of the work has been carried out in Technical Research Centre of Finland (VTT) and Fortum Nuclear Services Ltd.

References

ASME, 1990. Metal Fatigue in Operating Nuclear Power Plants—A Review of Design and Monitoring Requirements, Field Failure Experience, and Recommendations for ASME Section XI Action. Prepared by ASME Section XI Task Group on Fatigue in Operating Plants. Revision 0 (Draft), January 1990.

Becker, F.L., Doctor, S.R., Heasler, P.G., Morris, C.J., Pitman, S.G., Selby, G.P., Simonen, F.A., 1981. Integration of NDE Reliability and Fracture Mechanics—Phase I Report, NUREG/CR-1696 PNL-3469, vol. 1. 170 pp.

Hytönen, Y., 1998. Two leakages induced by thermal stratification at the Loviisa power plant. In: Proceedings of NEA/CSNI/R(98)8 Specialists' Meeting, Paris, France, 8–10 June, pp. 115–160.

Hänninen, H., Hakala, J., 1981. Pipe failure caused by thermal loading in BWR water conditions. Int. J. Pressure Vessel Piping 9, 445–455.

Iida, K., Takumi, K., Naruse, A., 1988. Influence of stress condition on flaw detectability and sizing accuracy by ultrasonic inspection. In: Proceedings of the 9th International Conference on Nondestructive Evaluation in the Nuclear Industry, Tokyo, Japan, 25–26 April, pp. 563–567.

Ogilvy, J.A., 1989. Model for the ultrasonic inspection of rough defects. Ultrasonics 27, 69–79.

Pirson, J., Roussel, G., 1998. Emergency core cooling system pipe crack incident at the Tihange unit 1 plant. In: Proceedings of NEA/CSNI/R(98)8 Specialists' Meeting, Paris, France, 8–10 June, pp. 103–114.

Saka, M., Fukuda, Y., 1991. NDT of closed cracks by ultrasonic propagation along the crack surface. NDT&E Int. 24 (4), 191–194.

Uddcomb Engineering AB, 1999. Testblock med Implanterade Defekter. Brochure from Uddcomb Engineering.

Virkkunen, I., 2001. Thermal Fatigue of Austenitic and Duplex Stainless Steels, Acta Polytechnica Scandinavica. Mechanical Engineering Series No. 154, Espoo, 115 pp. Available online at: (http://lib.hut.fi/Diss/2001/isbn9512256878/).

Virkkunen, I., Kemppainen, M., Hänninen, H., 2000. Residual stresses induced by cyclic thermal loads. In: Proceedings of the Sixth International Conference on Residual Stresses ICRS-6, Oxford, UK, 10–12 July, pp. 529–536.

Wåle, J., Ekström, P., 1995. Crack Characterisation for In-service Inspection Planning, SKI Projekt 14.4-940389, 94164 SAQ/FoU-Rapport 95/70, SAQ Kontroll AB, Stockholm, Sweden, 84 pp.

Watson, P., Edwards, R.L., 1996. Fabrication of test specimens simulating IGSCC for demonstration and inspection technology evaluation. In: Proceedings of the 14th International Conference on NDE in the Nuclear and Pressure Vessel Industries, Stockholm, Sweden, 24–26 September, pp. 165–168.

Wirdelius, H., Österberg, E., 2000. Study of Defect Characteristics Essential for NDT Testing Methods UT, EC and RT. SKI Project Number 98267, SKI Report 00/42, Sweden, 50 pp.

Yoneyama, H., Senoo, M., Miharada, H., Uesugi, N., 2000. Comparison of echo heights between fatigue crack and EDM-notch. In: Proceedings of the 2nd International Conference on NDE in Relation to Structural Integrity for Nuclear and Pressurized Components, New Orleans, Louisiana, USA, 24–26 May, 8 pp.